



Supplementary Materials for
Linear Complexions: Confined Chemical and Structural States at Dislocations

M. Kuzmina, M. Herbig, D. Ponge, S. Sandlöbes, D. Raabe

correspondence to: d.raabe@mpie.de

Materials and Methods

Synthesis and heat treatment

The Fe-9wt%Mn solid solution alloy was synthesized in a vacuum induction furnace and cast as a 4 kg rectangular billet from high purity ingredients (segregated edges of the slab were cut off), annealed at 1100 °C to homogenize the primary dendritic segregation in the solidification microstructure and then water quenched (Fig. S1). The alloy was cold rolled to 50% thickness reduction to increase the dislocation density. Additional long-time annealing promoting Mn diffusion was performed at (i) 400°C for 2 weeks (336 hours); (ii) 450°C for 6, 18 and 336 hours (2 weeks); and (iii) 540°C for 6 hours (Fig. S2). The nominal bulk composition was measured by wet chemical analysis (Table S1).

Characterization

We conducted detailed joint structural and chemical characterization by performing Atom Probe Tomography (APT) and Transmission Electron Microscopy (TEM) individually, as well as jointly on the same sample (correlative TEM/APT (*Error! Reference source not found.,Error! Reference source not found.*)).

Conical APT samples with tip radii < 100 nm were prepared using a FEI Helios NanoLab600i dual-beam Focused Ion Beam (FIB)/Scanning Electron Microscopy (SEM) instrument. APT was performed using a LEAP 3000X HR device by Imago Scientific Instruments at a set-point temperature of 50 K in laser mode with 532 nm wavelength, ~10 ps pulse width, 250 kHz pulse frequency and 0.4 nJ pulse energy. For reconstructing 3D atom maps, visualization and quantification of partitioning using proximity histograms (*Error! Reference source not found.*) which allow for mapping concentrations normal to iso-concentration surfaces (delocalization 2 nm, voxel size 0.7 nm, Mn iso-value 14 at%) the commercial software IVAS® by Imago was employed.

The bright and dark-field TEM investigations were conducted on electrochemically prepared samples in a Philips CM20 with a LaB₆ filament operated at 200 kV. Electron diffraction conducted on near-planar crystalline features, such as needle- or rod-shaped precipitates, may cause elongated diffraction signals instead of diffraction spots. For bulk crystals electron diffraction occurs for those sets of lattice planes which are in Bragg condition or close to it, i.e. a diffraction spot (“point”) is created. For extended, thin crystals, i.e. planar precipitates, the Ewald sphere is cut not only in Bragg condition but also close to the Bragg condition at the same time. This results in elongated diffraction signals, so-called streaks or rel-rods. This type of diffraction situation is expected for a complexion along a dislocation line. However, in the current analysis the diffraction intensity was too low for streaking to be observed owing to the tiny volume of the complexions as compared to the matrix.

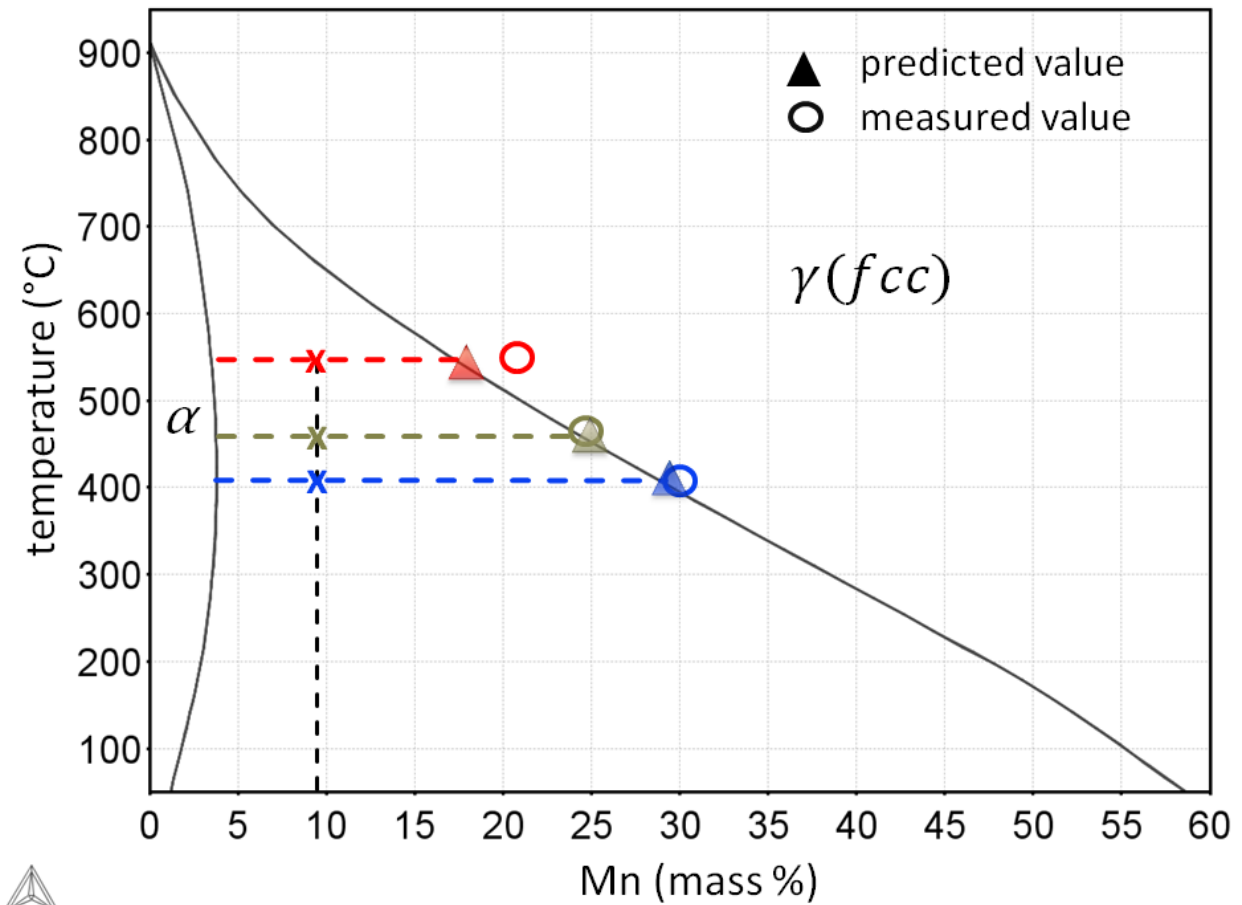
For the correlative TEM/APT experiments with an experimental setup described in (*Error! Reference source not found.,Error! Reference source not found.*) the specimens were extracted from the surface of the bulk material by standard FIB lift-out procedures, deposited on a bisected, electropolished TEM grid, sharpened to tip radii of <100 nm and subsequently analyzed first by TEM in a JEOL JEM-2200FS in STEM mode, operated at 200 kV and then by APT. Here, the STEM images were employed as templates to fine-tune the reconstruction parameters of the 3D atom maps.

Thermodynamic Calculations of Mn Partitioning

The equilibrium solubility of Mn in austenite was derived by using the ThermoCalc 4-0 software for the calculation of thermodynamic and phase equilibria according to the Calphad approach. We used the latest thermodynamic database TCFE7 for Fe alloys (*Error! Reference source not found.*).

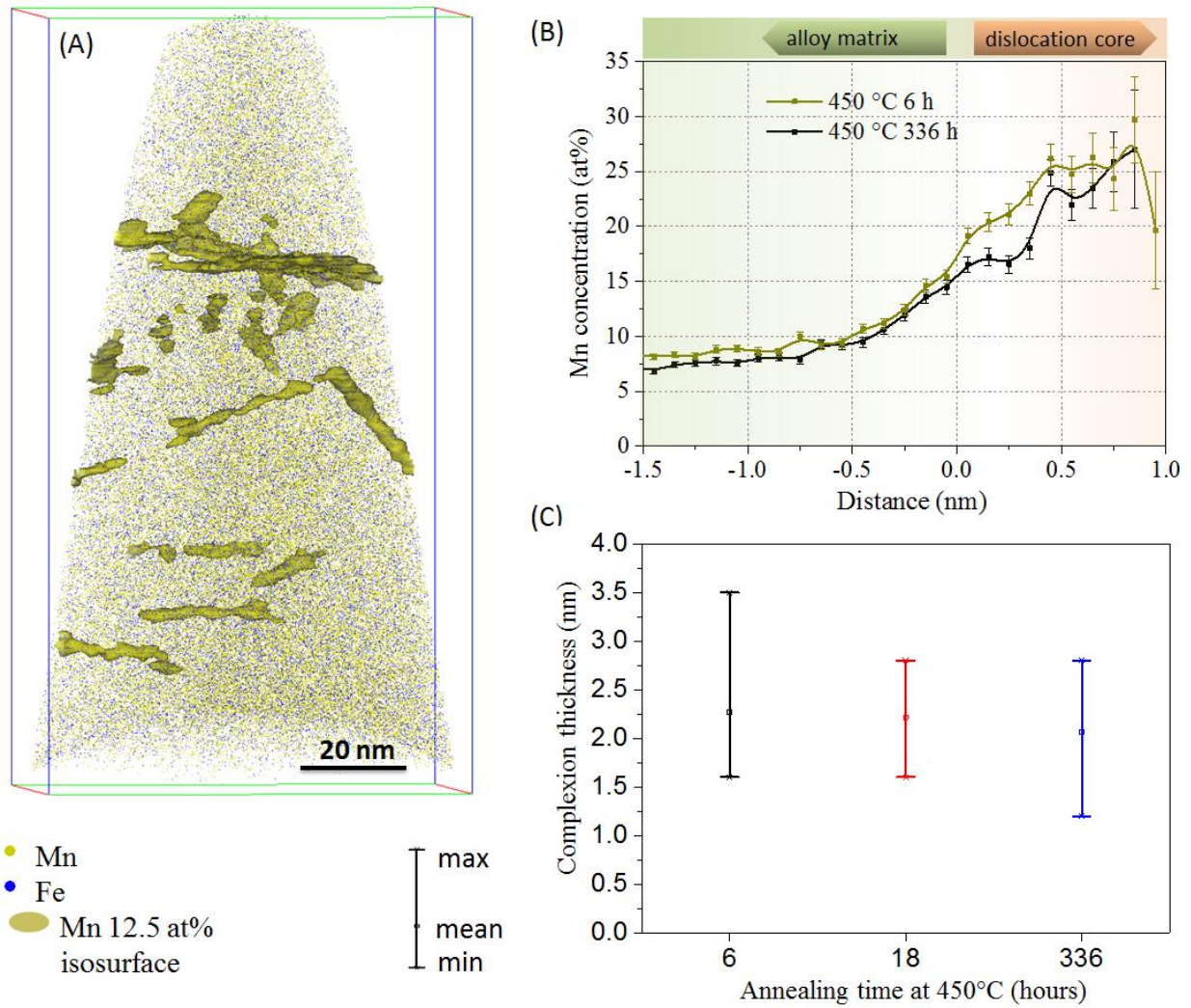
Calphad methods use all types of available measured and theoretically obtained data on phase equilibria and thermochemical constants in an alloy system. The thermodynamic properties of each phase are then described through the Gibbs free energy, applying a mathematical model in conjunction with adjustable parameters.

Fig. S1.



Supplemental Fig. S1. Fe-Mn equilibrium phase diagram. The phase diagram indicates three different heat treatment temperatures. The three annealing treatments lead to specific Mn partitioning ratios between the bcc matrix and the fcc states at the dislocation cores as analyzed in the atom probe experiments (open symbols). The Mn content observed experimentally inside the dislocations matches the equilibrium Mn content shown by the open symbols very well. Mass % is practically identical to at.% for Fe-Mn alloys. This finding confirms that the Mn-decorated dislocations form confined austenitic (γ , fcc) states inside an otherwise body centered cubic (α , bcc, martensitic) crystal.

Fig. S2



Supplemental Fig. SM2. Kinetic stability of the confined austenitic dislocation core states. (A) Atom probe tomography data set showing a number of dislocations with confined austenitic core regions (elongated green features marked by the Mn isosurface) after long-term annealing of 336 h at 450°C. (B) Proximity histograms performed using identical parameters on a sample aged for 6 hours and 336 hours at 450°C, respectively.

Prolonged aging neither affects size nor composition of the austenitic core regions which is one of the most characteristic features of complexions. (C) Overview diagram showing corresponding size data for the austenitic dislocation core regions for different annealing times at 450°C. The data reveal that the austenitic states remain unchanged also for very long annealing times.

Table S1.Table 1: Chemical composition of the bulk alloy in wt% according to wet-chemical analysis.

Mn	C	Ni	Co	Mo	Si	Al	S	P	O	N
8,46	0,0075	0,0175	0,0022	<0,002	0,0024	<0,002	0,0047	<0,002	0,0102	0,0040